Journal of Integrative Agriculture 2026, 25(9): 3692–3702

KeAi CHINESE ROOTS GLOBAL IMPACT

Available online at ScienceDirect

Journal of Integrative Agriculture

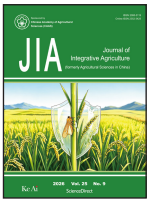

RESEARCH ARTICLE

The inhibition of photosynthesis and enhanced pigment degradation result in the variegated phenotype in tea leaves (*Camellia sinensis*)

Yifan Li, Huiyan Jia, Yafei Guo, Zuguo Xi, Yufei Wang, Mengqian Lu, Wei Tong, Qianying Dai, Weiwei Deng#

State Key Laboratory of Tea Plant Germplasm Innovation and Resource Utilization, Anhui Agricultural University, Hefei 230036, China

Highlights

- An ecologically insensitive variegated tea plant was identified.
- Inhibited expression of photosynthetic proteins reduces chlorophyll content.
- Variegated tea leaves undergo carbon starvation.
- Enhanced chlorophyll degradation causes leaf albinism in variegated tea plants.

Abstract

A novel variegated tea cultivar exhibiting a stable variegated phenotype was recently identified, demonstrating significantly elevated amino acid content concomitantly with reduced polyphenolic compound levels compared to conventional green-leaf varieties. Nevertheless, the underlying mechanism remains unclear. Here, variegated leaves and normal leaves of 'Huangshanzhong' tea plant were used to perform pigment content analysis and comparative transcriptome analysis. The chlorophyll content in variegated leaves significantly decreased compared to normal leaves, while the ratio of Chl *a* to Chl *b* was enhanced. Multiple genes (*CsrpiA*, *CsGAPDH*, *CsPGAM*, *CsPK* and *CsOGDH*) involved in sugar metabolism exhibited downregulated expression in variegated leaves. Key genes involved in the photosynthetic pathway were down-regulated in variegated leaves, including those encoding light-harvesting protein complex chlorophyll a/b binding proteins (*CsLhca1*, *CsLhca4*, *CsLhcb1* and *CsLhcb3*) and photosystem II complex proteins (*CspsbP* and *CspsbW*). Meanwhile, genes involved in chlorophyll degradation metabolism (*CsSGR* and *CsCLH1*) were upregulated in variegated leaves. Compared to the wild type, transgenic plants overexpressing *CsCLH1* and *CsCLH2* exhibited no significant changes in chlorophyll content. Enzyme activity assays showed that CsCLH1 could degrade chlorophyll *in vitro*. Subcellular localization results revealed that CsCLH1 and CsCLH2 were localized in the cytoplasm and nucleus. These findings suggest that impaired photosynthetic system function, suppressed carbohydrate synthesis, and accelerated degradation of photosynthetic pigments collectively contribute to the variegated phenotype in tea leaves. This study advances our understanding of mechanisms underlying leaf variegation in plants.

Keywords: *Camellia sinensis*, variegated phenotype, transcriptome, chlorophyll metabolism, photosynthesis

1. Introduction

Tea plant (*Camellia sinensis* (L.) O. Kuntze) is a perennial woody plant. Its leaves accumulate abundant bioactive metabolites such as theanine, catechins and caffeine, which endow tea with its characteristic flavor (Li *et al*. 2024). Tea not only exhibits significant application potential across various domains, including food and beverages, but also possesses essential health-care benefits. Notably, theanine has been shown to effectively promote relaxation both physically and mentally while alleviating stress (Turkozu and Sanlier 2017). In albino tea plants, the concentration of free amino acids often exhibits a significant upward trend, with a particularly notable increase in theanine content. Concurrently, there is a marked decrease in the levels of chlorophyll, carotenoids, catechins, and caffeine. These alterations in the concentrations of various substances impart unique biochemical characteristics to albino tea plants (Wei *et al.* 2012; Feng *et al.* 2014; Li *et al.* 2025). Nevertheless,

Received 11 May 2025; Received in revised form 28 June 2025; Accepted 30 July 2025; Available online 25 October 2025
#Correspondence Weiwei Deng, Tel/Fax: +86-551-65786401, E-mail: dengweiwei@ahau.edu.cn

doi: 10.1016/j.jia.2025.10.012

the molecular regulatory networks underlying albinism in tea plants remain insufficiently characterized.

According to the leaf color characteristics, albino tea plants can be classified into three types: albino, etiolated, and variegated (Zhang *et al.* 2020). Based on differences in environmental responsiveness, they are further categorized into two types: ecologically sensitive and ecologically insensitive (Zhang *et al.* 2020). The ecologically sensitive type demonstrates periodic albinism through climate-dependent mechanisms, categorized as either temperature-sensitive or light-sensitive subtypes. Temperature-sensitive cultivars exhibit an albino phenotype in spring when temperatures drop below 15°C, yet revert to a green phenotype at temperatures ranging from 22°C to 25°C (Wang *et al.* 2010; Li *et al.* 2019). Light-sensitive cultivars exhibit chlorosis under intense light exposure (greater than 15,000 lx). However, their leaves gradually revert to a green phenotype under conditions of reduced light intensity or shading (Liu *et al.* 2017; Tian *et al.* 2019). Tea plants characterized by variegated phenotypes, like 'Yanling Yinbiancha', belong to ecologically insensitive cultivars. They consistently exhibit variegated phenotypes, regardless of environmental fluctuations (Han *et al.* 2013; Ma *et al.* 2016; Gao *et al.* 2021).

In studies of albino tea plant, key genes involved in chlorophyll and carotenoid metabolic pathways have been identified to regulate photosynthetic pigment dynamics in albino leaves. *CsSGR* (*STAY-GREEN*) modulates leaf albinism through chlorophyll catabolism (Chen X F *et al.* 2022). The non-synonymous mutation from G to A in *CsCHLI* disrupts chlorophyll biosynthesis, determining an albino leaf trait of light-sensitive albino tea cultivar 'Baijiguan' (Zhang *et al.* 2024). The CsH1.2–*CsNYC1a* module regulates chlorophyll degradation to promote leaf whitening (Wu *et al.* 2024). Mutation of *phytoene desaturase* (*PDS3*) impedes chloroplast development at proplastid stage, leading to an albino phenotype (Qin *et al.* 2007).

Photosynthesis impairment is mechanistically linked to albinism in tea plant. Key photosystem components, including light-harvesting complex II chlorophyll *a*/*b*-binding proteins, exhibit expression patterns correlating with leaf whitening in albino cultivars (e.g., 'Xiaoxueya' and 'Huabai 1') (Du *et al.* 2009; Chen X F *et al.* 2022). In light-sensitive albino tea cultivar 'Huangjinya', photooxidative degradation of photosystem II (PSII) subunits induces chlorosis (Cai *et al.* 2022). Structural defects in chloroplasts compromise photosynthetic efficiency, inducing carbon limitation and metabolic reprogramming in albino plants (Li *et al.* 2020). For example, transcriptome profiling of 'Yanling Yinbiancha' has revealed predominant downregulation of energy metabolism-related differentially expressed genes (DEGs) in albino tissues (Li *et al.* 2019). In previous studies, there have been some investigations into the secondary metabolites of the variegated tea plant (Lu *et al.* 2022). However, the molecular mechanism of the formation of variegated tea leaves remains unclear.

In this study, transcriptome sequencing was conducted on the normal and variegated leaves of tea plants. System-level interrogation of pigment metabolism, photosynthesis, and carbohydrate metabolism revealed preliminary regulatory networks underlying variegation. Subsequent investigations considered *CsCLH1* and *CsCLH2* as chlorophyll catabolic regulators, with multidimensional functional validation analyzing their roles in chlorophyll degradation in tea plant. Integrated transcriptomic analyses provide mechanistic insights into leaf albinism in variegated tea plants, advancing our understanding of its molecular basis.

2. Materials and methods

2.1. Plant materials

Tea leaves were obtained from tea plants (*C. sinensis* cv. Huangshanzhong) in Furong Valley, Huangshan, Anhui, China in April 2021. The tea plant has both normal leaves (NL) and variegated leaves (VL). According to the various developmental stages of the leaves, they were systematically collected and classified. The first leaves of fresh shoots were named VLY and NLY, respectively. The second and third leaves of the tea plant were named VLM and NLM, respectively. The fifth to sixth leaves at the bottom of the tea branch were named VLO and NLO, respectively. All samples were immediately frozen in liquid nitrogen and then stored at –80°C for subsequent analyses. Five-week-old *Nicotiana benthamiana* plants were cultured in the greenhouse.

2.2. Determination of chlorophyll and carotenoid contents

A total of 1.0 g of fresh leaves without main veins was ground into powder and extracted in 10 mL of 95% ethanol for 24 h in the dark. After centrifugation for 10 min, the supernatant was analyzed using a U-5100 ultraviolet spectrophotometer (Hitachi, Tokyo, Japan) at A_{470}, A_{649}, and A_{665}. The contents of chlorophyll and carotenoids were calculated according to Wang *et al.* (2019).

2.3. Chloroplast ultrastructure analysis of normal and variegated tea leaves

Leaf segments (≈1 mm^2) were prepared according to Li *et al.* (2011). The samples were sectioned using a TCS CM1900 freezing microtome (Leica, Wetzlar, Germany) and stained *via* Daddow's protocol (Daddow 1983). Ultrastructural observations were conducted using a HT-7700 transmission electron microscope (Hitachi, Tokyo, Japan).

2.4. Expression profile of genes in pigment metabolism, photosynthesis, and sugar metabolism

Total RNA from VL or NL was isolated using the RNAprep Pure Plant Kit (Tiangen, Beijing, China). First-strand cDNA was synthesized using PrimeScript RT Master Mix (TaKaRa, Beijing, China). Quantitative real-time PCR (qRT-PCR) was performed using MonAm ChemoHS qPCR Mix (Monad, Wuhan, China). The internal reference gene was the actin gene (*CsACTIN1*, GenBank No. KA280216.1), and primers sequences were listed in Appendix A. The $2^{-\Delta Ct}$ method (Wu *et al.* 2016) was used to calculate relative expression. The experiment was performed with three biological replicates.

2.5. Cloning of *CsCLH1* and *CsCLH2*

Total RNA was extracted from VL using the RNAprep Pure

Plant Plus Kit (TIANGEN, Beijing, China). Subsequently, first-strand cDNA synthesis was performed with the MonScript™ RTIII Super Mix with dsDNase (Two-step) (Monad, Jiangsu, China). The resulting cDNAs served as templates for cloning the coding sequence of *CsCLH1* and *CsCLH2* using KOD One™ PCR Master Mix (TOYOBO, Shanghai, China).

2.6. Subcellular localization

The coding sequences of *CsCLH1* and *CsCLH2* were cloned into the pCAMBIA1305 vector to generate recombinant constructs, respectively. Recombinant plasmids (pCAMBIA1305-CsCLH1 and pCAMBIA1305-CsCLH2) were transformed into *Agrobacterium* GV3101, and positive clones were incubated at 28°C. The bacterial solution was resuspended and infiltrated into tobacco leaves. After two days, GFP signals were captured *via* Olympus FV1000 confocal microscope (Olympus, Tokyo, Japan). The empty vector served as control.

2.7. Transient overexpression in protoplasts of tea leaves

Young tea leaves were cut into thin strips, which were then immersed in a petri dish containing enzymatic solution. The composition of enzymatic buffer was determined according to the method described by Xu *et al.* (2021) with minor modifications. The mixture was hydrolyzed under a negative pressure of –0.1 kPa for 30 min, and then gently agitated at 25°C for 4 to 6 h. All mixtures were passed through a 50 μm cell strainer, followed by centrifugation and subsequent removal of the supernatant. The pellet was resuspended in 10 mL of W5 solution (0.4 mol L^{-1} mannitol, 5 mmol L^{-1} glucose, 125 mmol L^{-1} $CaCl_2$, 154 mmol L^{-1} NaCl, 2 mmol L^{-1} MES, and 5 mmol L^{-1} KCl, pH 5.7). After immersed in ice for 30 min, cells were purified in MMg buffer (0.4 mol L^{-1} mannitol, 4 mmol L^{-1} MES, and 15 mmol L^{-1} $MgCl_2$, pH 5.7). For transfection, 100 μL protoplast suspensions were mixed with recombinant plasmids (pCAMBIA1305-CsCLH1 and CsCLH2 or empty vector). Polyethylene glycol (PEG) 4000-mediated transformation was terminated with W5 solution. Transfected protoplasts were cultured in WI solution (0.5 mol L^{-1} mannitol, 4 mmol L^{-1} MES, 20 mmol L^{-1} KCl, pH 5.7) at 25°C for 16 h (dark conditions). GFP signals were captured using Olympus FV1000 confocal microscope (Olympus, Tokyo, Japan).

2.8. Transient overexpression in tobacco leaves

Agrobacterium GV3101 harboring pCAMBIA1305-CsCLH1, pCAMBIA1305-CsCLH2 or an empty vector (control) was infiltrated into tobacco leaves. Tobacco leaves were selected under similar growth conditions and leaf color for the experiment, which was conducted with three biological replicates. To observe phenotypic differences, one half of each leaf was injected with *Agrobacterium* GV3101, while the other half remained untreated. Three days later, treated leaves were collected, ground into powder in liquid nitrogen and used for chlorophyll content analysis and expression pattern analysis.

2.9. Western blot analysis

Western blot was performed using total proteins extracted from transgenic tobacco leaves of *CsCLH1* and *CsCLH2*. A total of 1.0 g of tobacco leaves was ground into powder in liquid nitrogen and homogenized in extraction buffer (50 mmol L^{-1} Tris, 1 mmol L^{-1} EDTA-2Na, 150 mmol L^{-1} NaCl, 5% glycerol, 1% triton-X-100, 1 mmol L^{-1} PMSF). The mixture was centrifuged for 10 min at 4°C. Proteins were resolved by SDS-PAGE, transferred to PVDF membranes, and probed with anti-actin (Sangon Biotech, Shanghai, China) and anti-GFP antibody (Zhengneng Biotechnology, Shanghai, China).

2.10. Overexpression of *CsCLH1* and *CsCLH2* in *Arabidopsis thaliana*

pCAMBIA1305-CsCLH1 and pCAMBIA1305-CsCLH2 were transferred into wild-type *A. thaliana* using floral-dip method (Wu *et al.* 2024), respectively. Positive strains were cultured and suspended in infiltration buffer consisting of 5% sucrose and 0.4‰ surfactant. The inflorescence was immersed in the infective solution for 30 s and then placed in darkness for 24 h. This process was repeated three times. Transgenic plants were screened on MS agar medium containing 30 mg L^{-1} hygromycin until homozygous lines were obtained.

2.11. Functional characterization of CsCLH1 *in vitro*

The coding sequence of *CsCLH1* was ligated to pGEX-4T-1. The construct was then transformed into *Escherichia coli* BL21 (DE3) (TransGen Biotech, Beijing). *Escherichia coli* BL21 (DE3) carrying pGEX-CsCLH1 and pGEX-4T-1 was cultured at 37°C until the OD_{600} reached 0.5–0.6. The culture was then induced with 0.05 mmol L^{-1} IPTG at 16°C for 20 h. Cells were ultrasonically lysed in 1× PBS buffer, and soluble fractions were purified by glutathione S-transferase (GST)-affinity chromatography (Sefinose™ 4FF) to obtain CsCLH1 protein. The protein concentration was determined using the Coomassie Brilliant Blue method.

Chlorophyll was extracted using the method described by Fukasawa *et al.* (2010). 200 μL of enzyme was mixed with 150 μL of chlorophyll (dissolved in acetone) and 650 μL of reaction buffer (100 mmol L^{-1} sodium phosphate, pH 7, and 0.24% Triton X-100) in the dark at 37°C for 1 h. The reaction was terminated by adding 1 mL of 10 mmol L^{-1} KOH. Then, the reaction solution was mixed with *n*-hexane and acetone (1:3:2). Chlorophyllase activity was detected and calculated according to Lu *et al.* (2022).

2.12. Statistical analysis

All data are shown as mean±standard deviation (SD; n=3). Data analysis was performed using Student's t-test for independent samples for two-group comparisons and one-way ANOVA followed by Duncan's multiple range test for multi-group comparisons. Asterisks indicate significance levels (*, $P \le 0.05$; **, $P \le 0.01$). Transcriptome data (Lu *et al.* 2022) were used to analyze the expression profile of genes involved in pigment metabolism, photosynthesis, and sugar metabolism. Figures were generated using GraphPad Prism 8.0.2, TBtools v 2.122 and R 4.5.1.

3. Results

3.1. Chlorophyll content decreased and chloroplast development was damaged in variegated leaves

VL and NL were collected from the same tea plant (Fig. 1-A and B). Variegated tea leaves displayed stable and environment-independent variegation that intensified with leaf maturation (Appendix B-a and c). Fresh leaves lacked visible variegation, presenting light-green pigmentation. As the leaves reached maturity, the variegated phenotype became more pronounced. The contents of chlorophyll *a* (Chl *a*) and chlorophyll *b* (Chl *b*) in VL were significantly lower than those in NL. The contents of Chl *a*, Chl *b*, and total chlorophyll in young leaves were all significantly lower than those in mature leaves. Although the above indices of mature leaves were slightly lower than those of old leaves, the differences were not statistically significant. In addition, no significant differences in carotenoid content were observed between NL and VL at different developmental stages (Fig. 1-C–E). The ratio of Chl *a* to Chl *b* was significantly higher in VL than in NL (Fig. 1-F).

Ultrastructural analysis revealed intact chloroplasts with normal thylakoid stacking in NL, contrasting with VL exhibiting stromal vacuolization and disorganized thylakoid architecture (Appendix B). These findings suggested that variegated tea leaves arise from synergistic chlorophyll deficiency and chloroplast structural anomalies.

3.2. KEGG enrichment analysis of DEGs across developmental stages revealed stage-specific metabolic perturbations

Pairwise comparisons (NLY *vs.* VLY, NLM *vs.* VLM, NLO *vs.* VLO) identified 1,708, 3,432, and 1,449 DEGs, respectively. In NLY *vs.* VLY, 'protein processing in the endoplasmic reticulum' and 'starch and sucrose metabolism' pathways showed maximal DEG enrichment, with 'DNA replication', 'monoterpenoid biosynthesis', and 'glucosinolate biosynthesis' being significantly enriched (Appendix C-a). NLM *vs.* VLM analysis highlighted 'metabolic pathways' and 'secondary metabolite biosynthesis' as top enriched categories, alongside 'linoleic acid metabolism', 'caffeine metabolism', and 'stilbenoid-diarylheptanoid, and gingerol biosynthesis' (Appendix C-b). NLO *vs.* VLO comparisons exhibited predominant enrichment in 'protein processing in the endoplasmic reticulum' and 'photosynthesis–antenna proteins' demonstrated the greatest level of enrichment (Appendix C-c). These findings indicated that leaf variegation in tea plant likely involves protein post-translational modifications regulating chloroplast-related pathways, including photosynthetic machinery and leaf metabolic networks.

3.3. Photosynthetic system proteins of variegated leaves were damaged

Comparative transcriptome analysis identified DEGs including genes encoding light-harvesting I complex chlorophyll a/b binding proteins (*CsLhca1* and *CsLhca4*), light-harvesting II complex chlorophyll a/b binding proteins (*CsLhcb1-1*, *CsLhcb1-2* and *CsLhcb3*), PS II subunit protein (*CspetH*), electron transport proteins (*CspsbW* and *CspsbP*), and F-type ATPases (*CsatpG-1* and *CsatpG-2*) (Fig. 2-A and B). The majority of DEGs were found to be downregulated in VL compared to NL. *CsLhca1* (TEA008963.1), *CsLhca4* (TEA008208.1), *CsLhcb1-1* (TEA019232.1), *CsLhcb1-2*

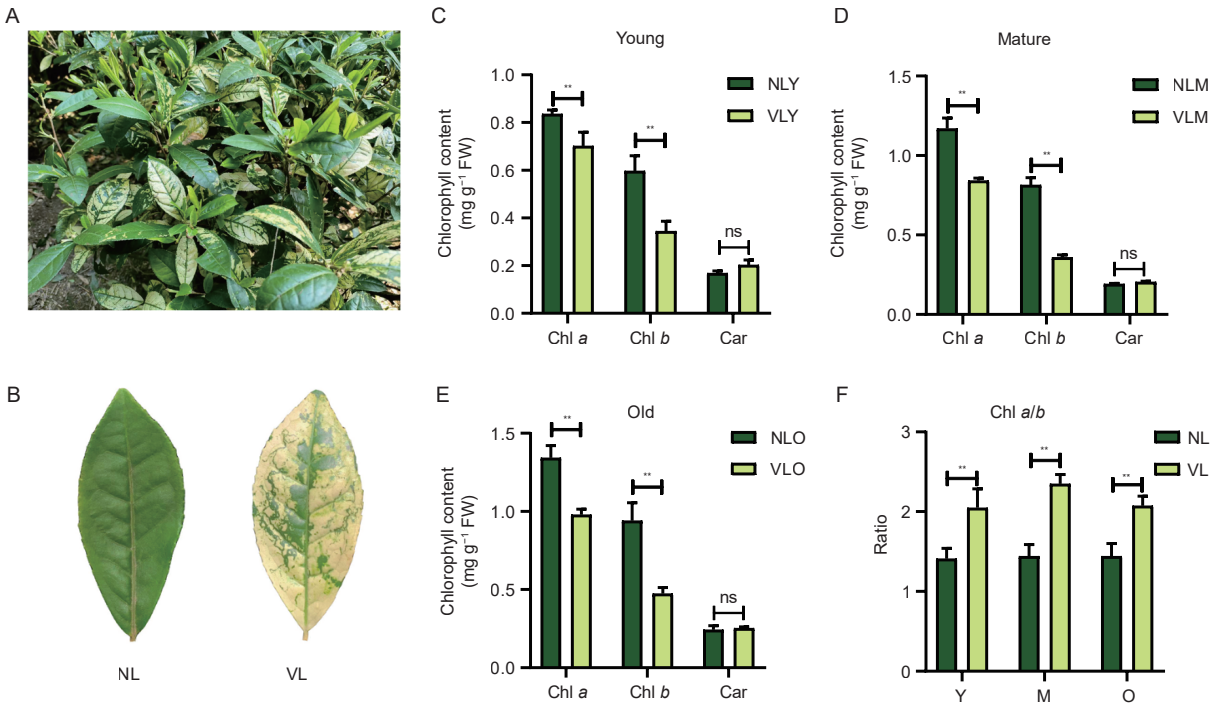

Fig. 1 The ecological phenotypes and pigment contents of variegated tea plants. A and B, appearance and phenotype of the variegated tea plant. C–F, photosynthetic pigment content and chlorophyll *a*/*b* ratio in normal leaves (NL) and variegated leaves (VL) across various developmental stages (Y, M and O, young, mature, and old leaves). ns, not significant; **, $P<0.01$.

(TEA001864.1), *CsLhcb3* (TEA017256.1) and the expression of *CsatpG-2* (TEA017141.1) were downregulated only during the senescence period, while *CspsbP* (TEA016728.1) and *CspsbW* (TEA005618.1) were downregulated in the young stage. Contrastingly, *CspetH* (TEA002093.1) and *CsatpG-1* (TEA022973.1) were upregulated during maturity. qRT-PCR validation confirmed photosynthetic gene expression profiles (Fig. 2-C). Correlation analysis revealed strong positive associations (R>0.8, P<0.05) between chlorophyll metrics and *CsatpG* (TEA017141.1), *CspsbP* (TEA016728.1), *CsLhca4* (TEA008208.1), and *CspsbW* (TEA005618.1) (Fig. 2-D).

3.4. Sugar metabolism was weakened in variegated tea leaves

Variegated tea leaves displayed impaired sugar metabolism across glycolysis, the pentose phosphate pathway (PPP), and the citric acid cycle (Fig. 3-A). Downregulation of *CsrpiA* (*ribose 5-phosphate isomerase A*) and *CsOGDH* (*2-oxoglutarate dehydrogenase*) was characterized in senescent leaves (Fig. 3-C), with PPP/citric cycle genes showing suppressed expression in VL. qRT-PCR validation revealed transcriptomic discrepancies, potentially reflecting spatiotemporal gene expression dynamics (Fig. 3-B). The results of the correlation analysis revealed that *CsOGDH* (BGI_novel_G000381), *CsPGAM-1* (TEA007732.1), *CsPGAM-2* (TEA021615.1) and *CsRPE* (TEA008221.1) exhibited a positive correlation with chlorophyll content (R>0.4, P<0.05). Conversely, *CsGAPDH* (TEA018881.1), *CsPK* (TEA023767.1), and *CsG6PD* (TEA024635.1) showed a negative correlation (|R|>0.4, P<0 .05) (Fig. 3-D).

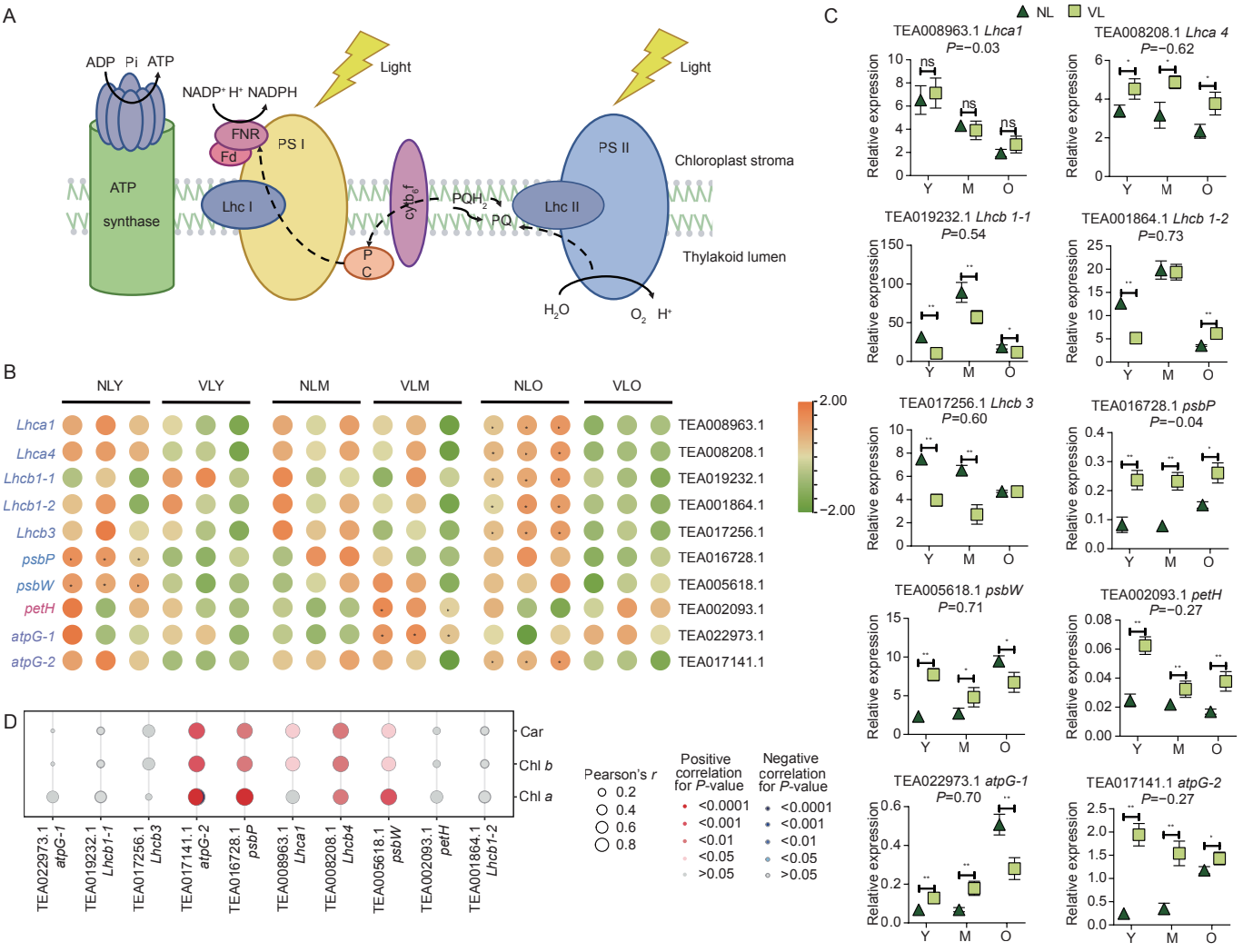

Fig. 2 Transcriptional regulation of photosynthetic pathway. A, schematic of photosynthetic electron transport chain. B, heatmap of DEGs in the photosynthesis. Lhca1/4, light-harvesting I chlorophyll *a*/*b* binding protein; Lhcb1/3, light-harvesting II chlorophyll *a*/*b* binding protein; psbW, photosystem II protein W; psbP, photosystem II protein P; petH, ferredoxin–NADP+reductase; atpG, ATPase subunit gamma. PS I, photosystem I; PS II, photosystem II; PQ, plastoquinone; Cyt b6/f, cytochrome b6/f; PC, plastocyanin; Fd, ferredoxin; FNR, ferredoxin-NADP+reductase. C, qRT-PCR validation of key DEGs. *, P<0.05; **, P<0.01. D, bubble chart displaying Pearson correlation coefficients between chlorophyll content and the expression of DEGs. The size of the bubbles indicates the r-value, with red representing a positive correlation and blue representing a negative correlation. The shade of each color reflects the P-value. NL, normal leaves; VL, variegated leaves; Y, M and O, young, mature, and old leaves.

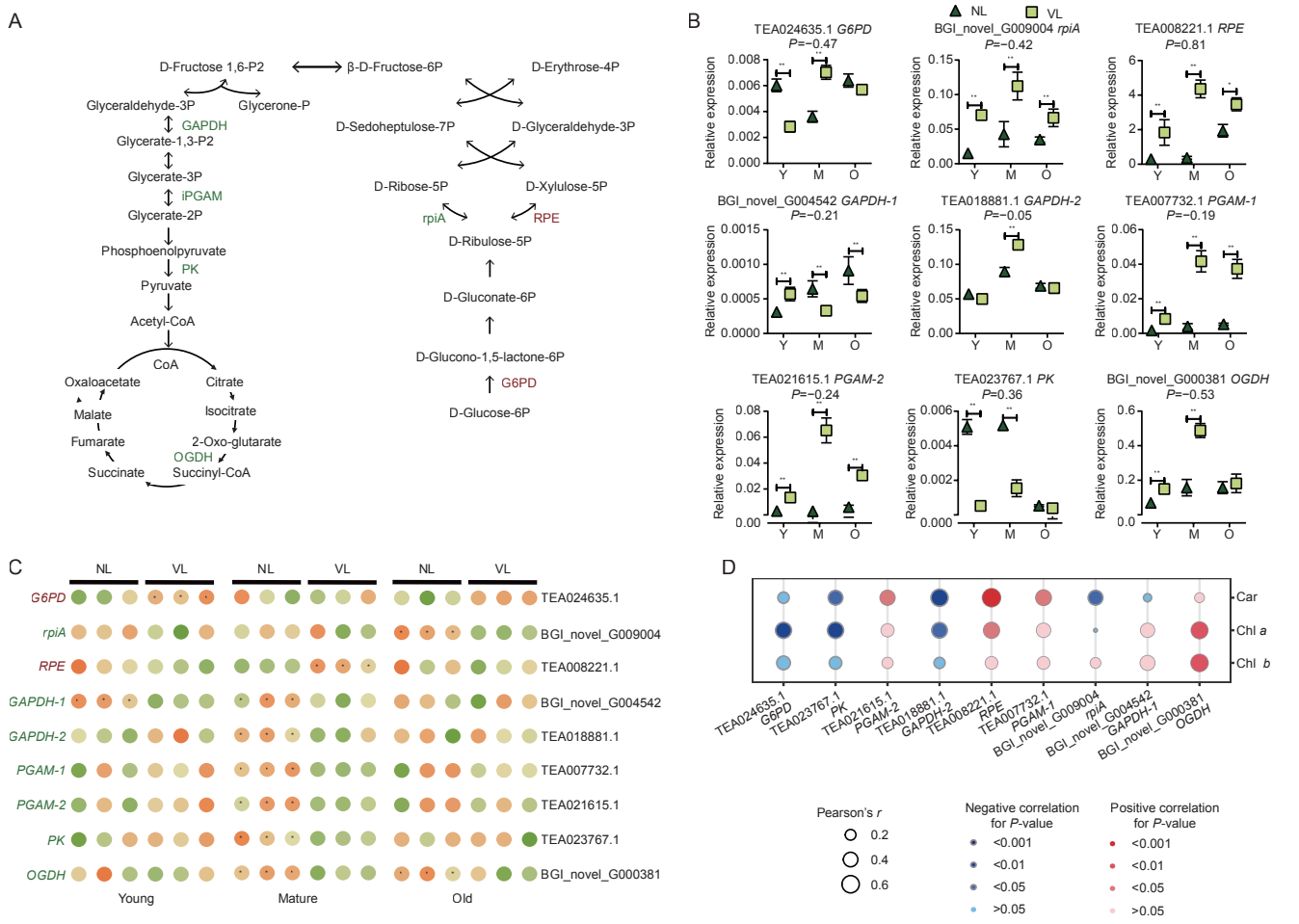

Fig. 3 Transcriptional regulation of sugar metabolism networks. A, model of the plant energy metabolism. B, qRT-PCR validation of key DEGs. *, $P<0.05$; **, $P<0.01$. C, heatmap of DEGs in the sugar metabolism. G6PD, glucose-6-phosphate 1-dehydrogenase; RPE, ribulose-phosphate 3-epimerase; rpiA, ribose 5-phosphate isomerase A; GAPDH, glyceraldehyde 3-phosphate dehydrogenase; PGAM, 2,3-bisphosphoglycerate-independent phosphoglycerate mutase; PK, pyruvate kinase; OGDH, 2-oxoglutarate dehydrogenase E1 component. D, bubble chart displaying Pearson correlation coefficients between chlorophyll content and the expression of DEGs. The size of the bubbles indicates the *r*-value, with red representing a positive correlation and blue representing a negative correlation. The shade of each color reflects the *P*-value. NL, normal leaves; VL, variegated leaves; Y, M and O, young, mature, and old leaves.

3.5. Expression patterns of DEGs in chlorophyll and carotenoid pathways

Among the DEGs in the carotenoid biosynthesis pathway (Fig. 4-A and C), it was observed that *CsZEP* was downregulated in VLM. As illustrated in Fig. 4-B and C, the DEGs in the chlorophyll metabolic pathway were primarily located downstream of synthesis, degradation, and cycle. These DEGs exhibited both upregulation and downregulation. The differential expression of these genes occurred predominantly during maturation and senescence. *CsCLH1* was significantly upregulated in the mature leaves, while Cs*SGR* was significantly upregulated in the old leaves. The downregulated genes were those encoding protochlorophyllide oxidoreductase (POR) and chlorophyllide *a* oxygenase (CAO). qRT-PCR was utilized to validate the expression of all DEGs across various growth stages. As shown in Fig. 4-D, there were some inconsistencies between the results of RNA-Seq and qRT-PCR. For instance, qRT-PCR results indicated that there were no significant differences in expression levels of *CsCAO* between VL and NL at various growth stages. *CsCLH1* was highly expressed in VLY and VLM, with senescent-stage attenuation. Except for specific down-regulation in VLO, the expression level of *CsCLH2* remained stable. Correlation analysis revealed a significant positive correlation between the expression pattern of *CsCLH1* and the chlorophyll content observed in different leaves ($P<0.05$ and $R>0.4$) (Fig. 4-E). Considering that *CsCLH2* and *CsCLH1* were paralogous genes, we also included *CsCLH2* in our research and conducted comprehensive investigations into its role.

3.6. Functional characterization of *CsCLH1* and *CsCLH2* in tobacco leaves

To investigate the functions of *CsCLH1* and *CsCLH2* in chlorophyll metabolism, transient overexpression experiments were performed in tobacco leaves. As shown in Fig. 5-A, the transgenic tobacco leaves did not exhibit an albino phenotype. The transcript levels of *CsCLH1* and *CsCLH2* in transgenic tobacco leaves were significantly upregulated

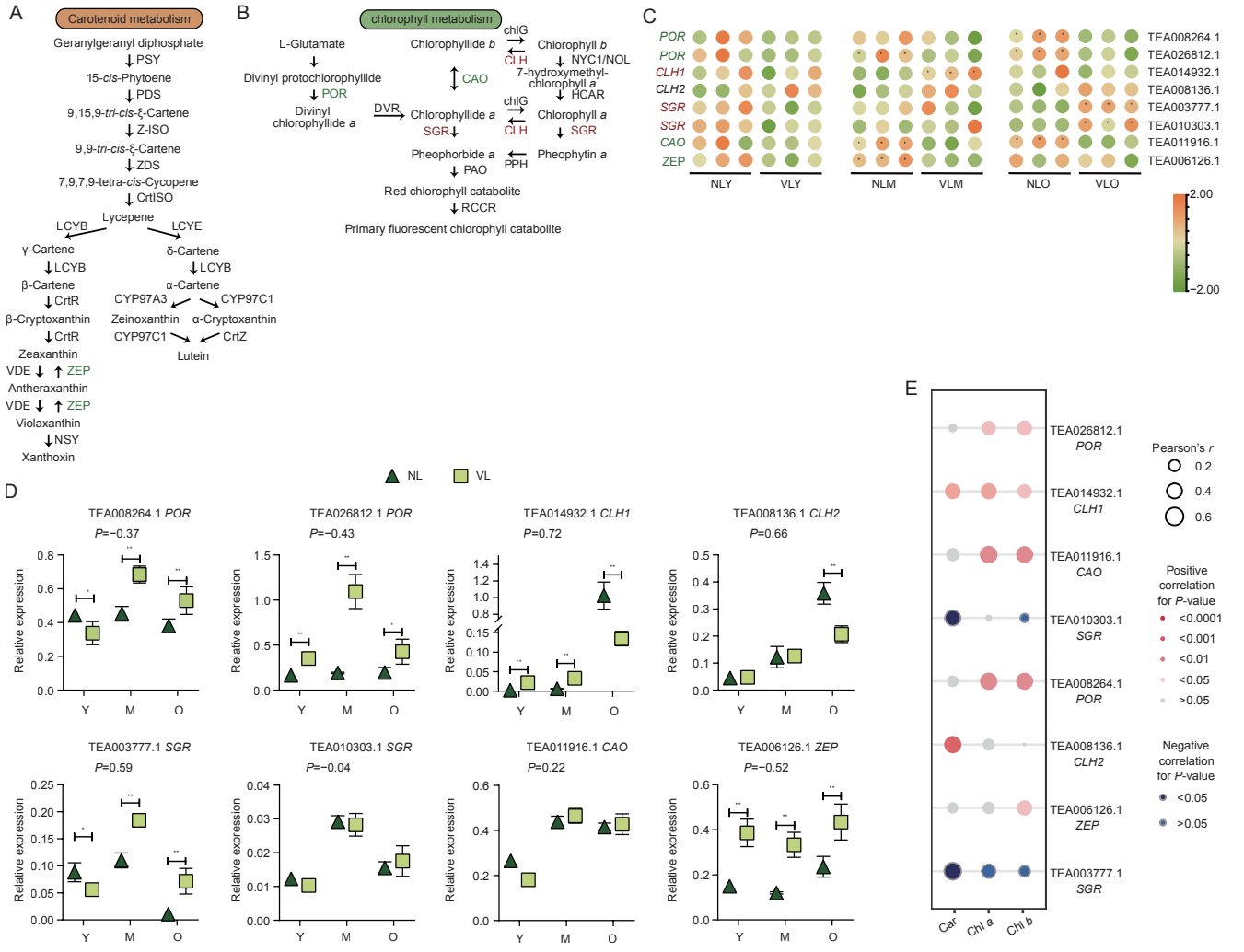

Fig. 4 Transcriptional regulation of photosynthetic pigment biosynthesis. A and B, flow diagram of carotenoid (A) and chlorophyll (B) metabolic pathways. The genes marked with colors are DEGs (red: upregulation, green: downregulation). POR, protochlorophyllide oxidoreductase; CAO, chlorophyllide *a* oxygenase; CLH, chlorophyllase; SGR, STAY-GREEN; ZEP, zeaxanthin epoxidase. C, heatmap of DEGs in the photosynthetic pigment biosynthesis. D, qRT-PCR validation of key DEGs. *, $P<0.05$; **, $P<0.01$. E, bubble chart displaying Pearson correlation coefficients of chlorophyll content and DEGs. The size of the bubbles indicates the *r*-value, with red representing a positive correlation and blue representing a negative correlation. The shade of each color reflects the *P*-value. NL, normal leaves; VL, variegated leaves; Y, M and O, young, mature, and old leaves.

relative to the control (Fig. 5-B). The western blot confirmed the protein level of CsCLH1 and CsCLH2 in transgenic tobacco leaves (approximately 59 kDa) (Fig. 5-D). However, the chlorophyll content in transgenic leaves overexpressing *CsCLH1* and *CsCLH2* did not change significantly compared with the controls (Fig. 5-C).

3.7. Functional characterization of *CsCLH1* and *CsCLH2* in *Arabidopsis*

To confirm the functions of *CsCLH1* and *CsCLH2* in tobacco leaves, we performed stable transformation of *CsCLH1* and *CsCLH2* in *Arabidopsis*. After 4 d of dark treatment, *CsCLH1*-OE and *CsCLH2*-OE lines exhibited phenotypic stability matching wild-type controls in leaf coloration (Fig. 5-E and I), chlorophyll content (Fig. 5-G and K) and photosynthetic efficiency metrics (F_v/F_m) (Fig. 5-F and J).

3.8. Purification and enzyme activity assay of CsCLH1 *in vitro*

To confirm the results of CsCLH1 in transgenic plants, assays of prokaryotic expression and enzyme activity analysis *in vitro* were performed. SDS-PAGE confirmed successful CsCLH1-GST fusion protein expression (approximately 58 kDa) (Fig. 5-H). Using chlorophyll extracted from spinach leaves as the reaction substrate, it was reacted with the highly concentrated CsCLH1 fusion protein. Interestingly, compared to the control group, CsCLH1 fusion protein exhibited significantly enhanced ability to degrade chlorophyll (Fig. 5-L).

4. Discussion

4.1. Chlorophyll content increases with the maturity of tea leaves

Studies have shown that leaf maturity significantly affects photosynthetic pigments dynamics, particularly chlorophyll

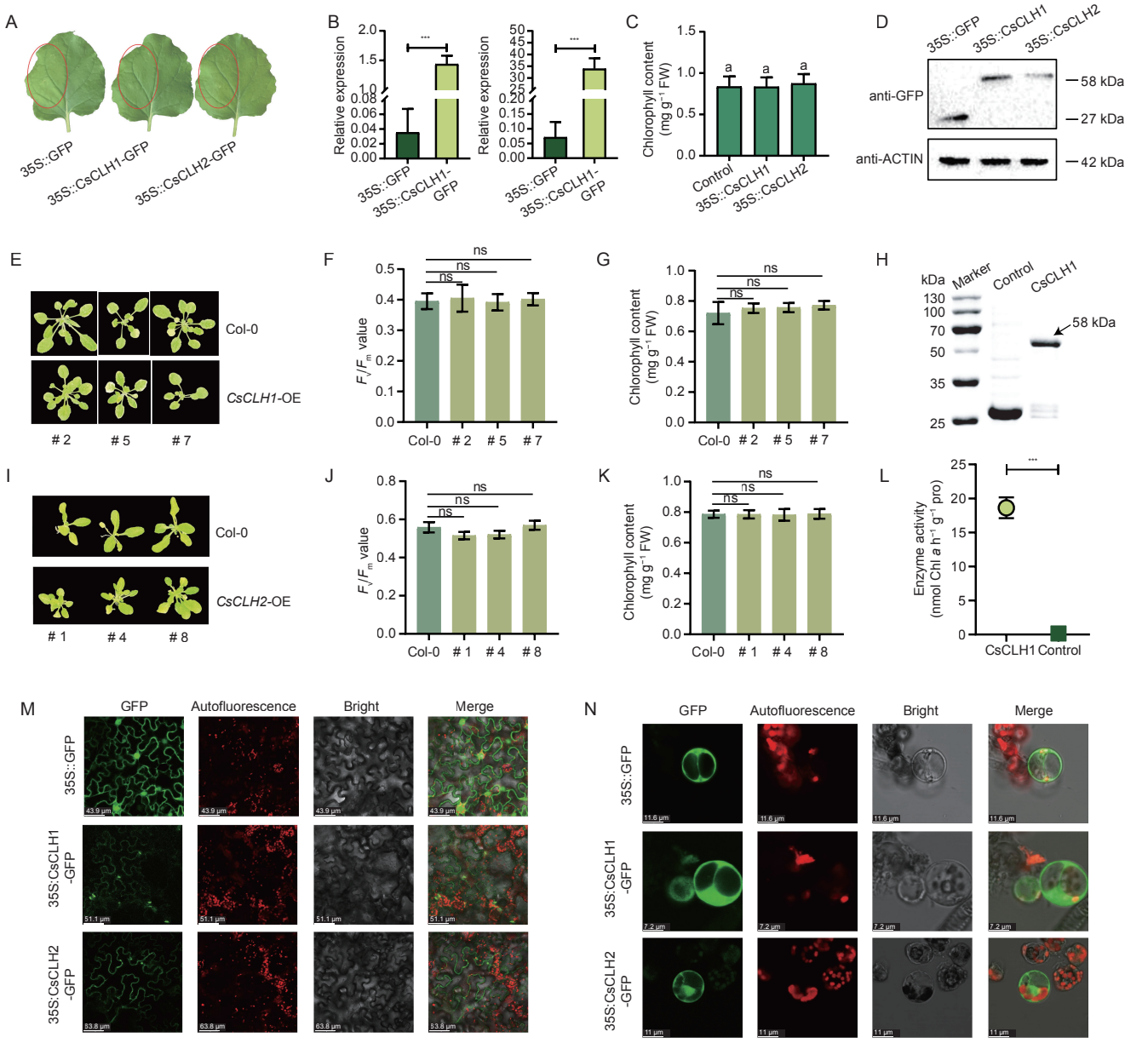

Fig. 5 Functional verification of *CsCLH1* and *CsCLH2*. A, phenotype of tobacco transiently overexpressing *CsCLH1* and *CsCLH2*. The injected region is shown in the red circle on the left side. B, qRT-PCR validation of *CsCLH1* and *CsCLH2* expression. C, determination of chlorophyll content. D, Western blot analysis of CsCLH1 and CsCLH2. E–G and I–K, dark-induced senescence phenotypes (E, I), F_v/F_m value (F, J) and chlorophyll content (G, K) of wild-type (WT) and *CsCLH1*-OE and *CsCLH2*-OE *Arabidopsis*. H, purification of recombinant CsCLH1 (SDS-PAGE). L, enzymatic activity assay of CsCLH1. ns, not significant; **, $P<0.01$. M and N, subcellular localization of CsCLH1 and CsCLH2 in *N. benthamiana* (M) and *Camellia sinensis* (N).

accumulation (Cantwell *et al.* 2022). Research on 'Baiye 1' and 'Longjing 43' has demonstrated that chlorophyll content significantly increases with leaf maturation and then tends to flatten out (Wang 2011; Li *et al.* 2018). The same result was also obtained in the study of *Ailanthus altissima* (Zheng *et al.* 2023). Moreover, when measuring chlorophyll contents in the first to sixth leaves between the apical bud and fish leaf of new shoots of cultivars 'Huangdan' and 'Chunxuan', the chlorophyll content exhibited a fluctuating downward trend. This indicates that the change in chlorophyll content of tea leaves is related to maturity, while leaf position is not a decisive factor (Wang *et al.* 2016). This pattern is consistent with the change trend of chlorophyll content with maturity in VL and NL (Fig. 1-D and E). Wang *et al.* (2016) investigated the carotenoid content in tea leaves across different leaf positions in five tea varieties and observed that the levels exhibited irregular fluctuations. Similarly, this was consistent with the carotenoid content results in VL and NL.

4.2. Photosystem impairment drives leaf albinism

As shown in Fig. 2-A, the four major photosynthetic complexes of plants, including PSII, PSI, cytochrome b6/f (cytb6/f) complex and plastid ATP synthase, are located on the chloroplast thylakoid membrane (Croce and van Amerongen

2014). Light-harvesting complex (LHC) plays a crucial role as an antenna protein in the photosynthetic system of higher plants. LHCI and LHCII form complexes with PSI and PSII (PSI-LHCI and PSII-LHCII) to harvest light energy through the bound Chl *a* and Chl *b* (Levin and Schuster 2023). The core complex of PSII consists of 20 protein subunits. The degradation of PS II subunits adversely affects the structure and function of thylakoid membranes. Thylakoid membrane serves as a crucial site for the light reactions of photosynthesis, and any structural damage to thylakoids disrupts normal photosynthetic light reactions, ultimately resulting in leaf albinism (Cai *et al.* 2022). Therefore, photosynthetic system impairment results in the dissociation of chlorophyll from its complex, impairing its ability to effectively capture, transfer, and convert light energy. Consequently, the light reaction process of photosynthesis is significantly inhibited. Free chlorophyll becomes susceptible to external environmental factors and intracellular enzymes, which accelerates its degradation and ultimately leads to an albino phenotype. In variegated leaves, LHC and PSII-associated genes (*CsLhca1*, *CsLhca4*, *CsLhcb1-1*, *CsLhcb1-2*, *CsLhcb3*, *CspsbP*, *CspsbW* and *CsatpG-2*) were significantly down-regulated (Fig. 2-B). This indicated that the expression of photosynthesis and antenna proteins was inhibited. Ma *et al.* (2016) discovered that the decrease in abundance of photosynthetic proteins may be associated with the leaf color of tea plants. It suggests that photosystem impairment promotes chlorophyll loss. Moreover, this finding is consistent with results regarding 'Yanlingyinbiancha' (Gao *et al.* 2021).

4.3. Variegated leaf chlorosis correlates with sugar metabolism dysfunction

Sugar metabolism plays a pivotal role in plant growth, particularly in energy supply. In albino leaves, the development of the photosynthetic system is disrupted, and chlorophyll synthesis is restricted while degradation is accelerated, thereby rendering the light reaction unable to proceed normally. Previous studies have shown that albino tissues may obtain energy by absorbing sucrose from green tissues, thereby providing the driving force for their growth and development (Aluru *et al.* 2009; Gao *et al.* 2021). Analysis of the transcriptome data indicated several genes encoding key enzymes in the glycolytic pathway and the TCA cycle, such as *CsrpiA*, *CsGAPDH*, *CsPK*, *CsOGDH* and *CsPGAM* were found to be downregulated in the VL (Fig. 3-B). Therefore, VL exhibited impaired carbohydrate partitioning due to chlorophyll metabolism dysfunction. In contrast, the expressions of *CsG6PD* and *CsRPE* were upregulated in VL (Fig. 3-B). G6PD serves as the key rate-limiting enzyme in the pentose phosphate pathway (Stincone *et al.* 2015; Chen P H *et al.* 2022). The upregulation of *CsG6PD* suggested an increased oxidation of pentose phosphate in VL, indicating the higher demand for green tissue producing more energy to support albino tissue in variegated leaves.

4.4. The Inhibition of photosynthetic pigments accumulation led to albino tea leaves

Phytopigment homeostasis disruption drives leaf albinism through dual-phase regulation: chlorophyll biogenesis inhibition and catabolic activation (Li *et al.* 2019). Studies on 'Huangjinya', 'Baijiguan', and 'Yanlingyinbiancha' have indicated an association between the albino phenotype and reduced chlorophyll content (Li *et al.* 2016, Wu *et al.* 2016, Gao *et al.* 2021). The chlorophyll *a*/*b* ratio was found to be higher in VL than in NL, which is consistent with previous studies on albino tea cultivars 'Huangjinya' and 'Jibai' (Chen *et al.* 2024). The expression of *CsPOR*, which encodes a key enzyme in chlorophyll synthesis, was lower in VL. The silencing of Cs*POR1* in tea leaves through VIGS (Virus-Induced Gene Silencing) technology led to leaf albinism (Li *et al.* 2023). It was observed that the overexpression of *PORA* led to the restoration of chlorophyll synthesis and the normal phenotype (Paddock *et al.* 2010). Thus, the down-regulation of chlorophyll content in VL may be related to the down-regulation of *CsPOR*. SGR plays a key role in chlorophyll degradation. In 'Huabai 1', the expression of *CsSGR* was higher in albino tea leaves, and overexpression of *CsSGR* led to obvious albino phenotype in transgenic plants (Chen X F *et al.* 2022). Similar functions of *SGR* were also observed in *Arabidopsis* and *Oryza sativa* (Park *et al.* 2007; Sakuraba *et al.* 2012). In the present study, the expression of *CsSGR* (TEA003777.1 and TEA010303.1) were up-regulated in VL. We also found that the gene *CsCLH1* (TEA014932.1) encoding the chlorophyllase in the chlorophyll degradation pathway were significantly upregulated in VL (Fig. 4-C). This indicated that *CsSGR* is highly likely to regulate the content of chlorophyll in VL. Chlorophyllase is capable of breaking down chlorophyll into chlorophyllide and phytol (Hortensteiner 2006). Tsuchiya *et al.* (1999) expressed the gene products of *AtCLH1* and *CaCLH* in *E. coli*, and their purified proteins were capable of demonstrating chlorophyll-degrading activity. Integrated evidence establishes that chlorophyll depletion in variegated leaves arises from coordinated biosynthetic suppression and catabolic activation of photosynthetic pigments.

4.5. Chlorophyllase localization limits its role in chlorophyll degradation

The function and subcellular localization of chlorophyllase remain debated in plants. Given that chlorophyll predominantly exists in thylakoid membrane-protein complexes, with minor amounts in the stroma, the mechanism of chlorophyllase–substrate interaction and subsequent degradation requires further investigation. While chlorophyllase localization on the chloroplast envelope has been reported in *citrus* and other species (Hirschfeld and Goldschmidt 1983; Matile *et al.* 1997; Okazawa *et al.* 2006; Harpaz-Saad *et al.* 2007; Shemer *et al.* 2008), studies in *Arabidopsis* suggest its localization occurs outside chloroplasts (Schenk *et al.* 2007; Hu *et al.* 2015). These results indicate that CLH may not directly mediate endogenous chlorophyll degradation. In this study, overexpressing *CsCLH1* and *CsCLH2* in tobacco and tea mesophyll cells yielded results consistent with Arabidopsis observations (Fig. 5-M and N), further supporting non-essential role of chlorophyllase in endogenous chlorophyll degradation in VL. Chlorophyllase extracted from *citrus* and *Arabidopsis*

can degrade chlorophyll to produce chlorophyllide *in vitro* (Benedetti and Arruda 2002; Kariola *et al.* 2005; Harpaz-Saad *et al.* 2007). The same result was obtained in our study. Although the CsCLH1 protein expressed in a prokaryotic system was capable of degrading chlorophyll *in vitro* (Fig. 5-H and L), transgenic plants expressing *CsCLH1* and *CsCLH2* did not exhibit chlorophyll degradation (Fig. 5-E–G; I–K). This lack of degradation was likely due to the inability of chlorophyllase and its substrate to directly interact within variegated tea plants. This is consistent with the results of research on the function of chlorophyllase in *A. thaliana* (Schenk *et al.* 2007, Hu *et al.* 2015). *CsCLH1* isolated from the young tea leaves (*C. sinensis* cv. Shuchazao) enhances chlorophyll catabolism (Liu *et al.* 2023), potentially through natural variations distinguishing it from variegated cultivars.

5. Conclusion

To investigate the potential causes for variegated phenotypes in tea plants, we conducted an analysis of the transcriptome data of VL and NL. We selected DEGs associated with chlorophyll and carotenoid metabolism, the photosynthesis, and sugar metabolism. The results showed the inhibition of photosynthesis might lead to lower chlorophyll content. It appeared that the variegated leaves suffered a carbon starvation condition, and it is likely that the supply of sucrose in albino tea tissues could come from the green tissues of the leaf. It seems that the inhibition of photosynthetic pigments accumulation, coupled with the enhancement of degradation, probably contributed to the albino phenotype of variegated leaves. Although chlorophyllases can degrade chlorophyll *in vitro*, they exert no essential function in endogenous chlorophyll breakdown in planta. This study lays a solid foundation for further research on the molecular regulatory mechanism of variegated tea leaves.

Acknowledgements

This study was supported by the National Key Research and Development Program of China (2021YFD1601103), the National Natural Science Foundation of China (NSFC, 32573081), the earmarked fund for the China Agriculture Research System (CARS-19) and the Anji Baicha Tea Resource Comprehensive Utilization Research Center, China.

Declaration of competing interest

The authors declare that they have no conflict of interest.

Declaration of generative AI and AI-assisted technologies in the writing process

During the preparation of this manuscript, the authors used DeepSeek to assist in improving the clarity and readability of the language. All content generated was carefully reviewed and revised by the authors as necessary, and the authors take full responsibility for the final content of the article.

Appendices associated with this paper are available at https://doi.org/10.1016/j.jia.2025.10.012

References

Aluru M R, Zola J, Foudree A, Rodermel S R. 2009. Chloroplast photooxidation-induced transcriptome reprogramming in Arabidopsis *immutans* white leaf sectors. *Plant Physiology*, **150**, 904–923.

Benedetti C E, Arruda P. 2002. Altering the expression of the chlorophyllase gene *ATHCOR1* in transgenic Arabidopsis caused changes in the chlorophyll-to-chlorophyllide ratio. *Plant Physiology*, **128**, 1255–1263.

Cai W H, Zheng X Q, Liang Y R. 2022. High-light-induced degradation of photosystem II subunits' involvement in the albino phenotype in tea plants. *International Journal of Molecular Science*, **23**, 8522.

Cantwell M I, Hong G, Albornoze K, Berlanga M. 2022. Fresh grapevine (*Vitis vinifera* L.) leaves: Postharvest biology and handling recommendations. *Scientia Horticulturae*, **292**, 110627.

Chen P H, Tjong W Y, Yang H C, Liu H Y, Stern A, Chiu D T Y. 2022. Glucose-6-phosphate dehydrogenase, redox homeostasis and embryogenesis. *International Journal of Molecular Sciences*, **23**, 2017.

Chen X F, Li J J, Yu Y, Kou X B, Periakaruppan R, Chen X, Li X H. 2022. *STAY-GREEN* and *light-harvesting complex II chlorophyll a/b binding protein* are involved in albinism of a novel albino tea germplasm 'Huabai 1'. *Scientia Horticulturae*, **293**, 110653.

Chen Y J, Han Y X, He S Q, Cheng Q H, Tong H R. 2024. Differential metabolic profiles of pigment constituents affecting leaf color in different albino tea resources. *Food Chemistry*, **46**, 142290.

Croce R, van Amerongen H. 2014. Natural strategies for photosynthetic light harvesting. *Nature Chemical Biology*, **10**, 492–501.

Daddow L Y. 1983. A double lead stain method for enhancing contrast of ultrathin sections in electron microscopy: A modified multiple staining technique. *Journal of Microscopy*, **129**, 147–153.

Du Y Y, Shin S, Wang K R, Lu J L, Liang Y R. 2009. Effect of temperature on the expression of genes related to the accumulation of chlorophylls and carotenoids in albino tea. *Journal of Horticultural Science & Biotechnology*, **84**, 365–369.

Feng L, Gao M J, Hou R Y, Hu X Y, Zhang L, Wan X C, Wei S. 2014. Determination of quality constituents in the young leaves of albino tea cultivars. *Food Chemistry*, **155**, 98–104.

Fukasawa A, Suzuki Y, Terai H, Yamauch N. 2010. Effects of postharvest ethanol vapor treatment on activities and gene expression of chlorophyll catabolic enzymes in broccoli florets. *Postharvest Biology and Technology*, **55**, 97–102.

Gao X Z, Zhang C Y, Lu C, Wang M H, Xie N C, Chen J J, Li Y F, Chen J H, Shen C W. 2021. Disruption of photomorphogenesis leads to abnormal chloroplast development and leaf variegation in *Camellia sinensis*. *Frontiers in Plant Science*, **12**, 720800.

Han Z, Wang K, Deng L, Ming L I, Zhang L J. 2013. Albino tea cultivars-Huangjinban. *Tea*, **39**, 125–126. (in Chinese)

Harpaz-Saad S, Azoulay T, Arazi T, Ben-Yaakov E, Mett A, Shiboleth Y M, Hortensteiner S, Gidoni D, Gal-On A, Goldschmidit E, Eyal Y. 2007. Chlorophyllase is a rate-limiting enzyme in chlorophyll catabolism and is posttranslationally regulated. *Plant Cell*, **19**, 1007–1022.

Hirschfeld K R, Goldschmidt E E. 1983. Chlorophyllase activity in chlorophyll-free citrus chromoplasts. *Plant Cell Reports*, **2**, 117–118.

Hortensteiner S. 2006. Chlorophyll degradation during senescence. *Annual Review of Plant Biology*, **57**, 55–77.

Hu X Y, Makita S, Schelbert S, Sano S, Ochiai M, Tsuchiya T, Hasegawa S F, Hortensteiner S, Tanaka A, Tanaka R. 2015. Reexamination of chlorophyllase function implies its involvement in defense against chewing herbivores. *Plant Physiology*, **167**, 660–670.

Kariola T, Brader G, Li J, Tapio Palva E. 2005. Chlorophyllase 1, a damage control enzyme, affects the balance between defense pathways in plants. *Plant Cell*, **17**, 282–294.

Li C F, Ma J Q, Huang D J, Ma C L, Jin J Q, Yao M Z, Chen L. 2018. Comprehensive dissection of metabolic changes in albino and green tea cultivars. *Journal of Agricultural and Food Chemistry*, **66**, 2040–2048.

Li G D, Li Y, Yao X Z, Lu L T. 2023. Establishment of a Virus-Induced Gene-Silencing (VIGS) system in tea plant and its use in the functional analysis of *CsTCS1*. *International Journal of Molecular Sciences*, **24**, 14.

Li M Z, Wang W Z, Wang Y R, Guo L L, Liu Y J, Jiang X L, Gao L P, Xia T. 2024. Duplicated chalcone synthase (CHS) genes modulate

flavonoid production in tea plants in response to light stress. *Journal of Integrative Agriculture*, **23**, 1940–1955.
Li N N, Lu J L, Li Q S, Zheng X Q, Wang X C, Wang L, Wang Y C, Ding C Q, Liang Y R, Yang Y J. 2019. Dissection of chemical composition and associated gene expression in the pigment-deficient tea cultivar 'Xiaoxueya' reveals an albino phenotype and metabolite formation. *Frontiers in Plant Science*, **10**, 1543.
Li N N, Yang Y P, Ye J H, Lu J L, Zheng X Q, Liang Y R. 2016. Effects of sunlight on gene expression and chemical composition of light-sensitive albino tea plant. *Plant Growth Regulation*, **78**, 253–262.
Li Q, Huang J N, Liu S Q, Li J, Yang X H, Liu Y S, Liu Z H. 2011. Proteomic analysis of young leaves at three developmental stages in an albino tea cultivar. *Proteome Science*, **9**, 44.
Li Y F, Han Z, Wang M, Yan Y X, Ma R H, Wang H P, Deng W W. 2025. Metabolomics and sensory evaluation reveal the influence of four albino tea cultivars on the quality of processed green tea. *Food Research International*, **209**, 116180.
Li Y R, Li W J, Hu D, Shen P, Zhang G H, Zhu Y. 2020. Comparative analysis of the metabolome and transcriptome between green and albino zones of variegated leaves from *Hydrangea macrophylla* 'Maculata' infected by hydrangea ringspot virus. *Plant Physiology and Biochemistry*, **157**, 195–210.
Liu W M, Liu S Y, Zhang K Y, Xie M W, Sun H W, Huang X Q, Zhang L X, Li M. 2023. Chlorophyllase is transcriptionally regulated by CsMYB308/CsDOF3 in young leaves of tea plant. *Horticultural Plant Journal*, **9**, 1162–1176.
Levin G, Schuster G. 2023. LHC-like proteins: The guardians of photosynthesis. *International Journal of Molecular Sciences*, **24**, 2503.
Liu G F, Han Z X, Feng L, Gao L P, Gao M J, Gruber M Y, Zhang Z L, Xia T, Wan X C, Wei S. 2017. Metabolic flux redirection and transcriptomic reprogramming in the albino tea cultivar 'Yu-Jin-Xiang' with an emphasis on catechin production. *Science Reports*, **7**, 45062.
Lu M Q, Li Y F, Jia H Y, Xi Z G, Gao Q J, Zhang Z Z, Deng W W. 2022. Integrated proteomics and transcriptome analysis reveal a decreased catechins metabolism in variegated tea leaves. *Science Horticulturae*, **295**, 110824.
Ma C Y, Cao J X, Li J K, Zhou B, Tang J C, Miao A Q. 2016. Phenotypic, histological and proteomic analyses reveal multiple differences associated with chloroplast development in yellow and variegated variants from *Camellia sinensis*. *Scientific Reports*, **6**, 33369.
Matile P, Schellenberg M, Vicentini F. 1997. Localization of chlorophyllase in the chloroplast envelope. *Planta*, **201**, 96–99.
Okazawa A, Tango L, Itoh Y, Fukusaki E, Kobayashi A. 2006. Characterization and subcellular localization of chlorophyllase from *Ginkgo biloba*. *Zeitschrift Für Naturforschung C — A Journal of Biosciences*, **61**, 111–117.
Paddock T N, Mason M E, Lima D F, Armstrong G A. 2010. Arabidopsis protochlorophyllide oxidoreductase A (PORA) restores bulk chlorophyll synthesis and normal development to a *porB porC* double mutant. *Plant Molecular Biology*, **72**, 445–457.
Park S Y, Yu J W, Park J S, Li J, Yoo S C, Lee N Y, Lee S K, Jeong S W, Seo H S, Koh H J, Jeon J S, Park Y I, Paek N C. 2007. The senescence-induced staygreen protein regulates chlorophyll degradation. *Plant Cell*, **19**, 1649–1664.
Qin G J, Gu H Y, Ma L G, Peng Y B, Deng X W, Chen Z L, Qu L J. 2007. Disruption of phytoene desaturase gene results in albino and dwarf phenotypes in *Arabidopsis* by impairing chlorophyll, carotenoid, and gibberellin biosynthesis. *Cell Research*, **17**, 471–482.
Turkozu D, Sanlier N. 2017. L-theanine, unique amino acid of tea, and its metabolism, health effects, and safety. *Critical Reviews in Food Science and Nutrition*, **57**, 1681–1687.
Sakuraba Y, Schelbert S, Park S Y, Han S H, Lee B D, Andres C B, Kessler F, Hortensteiner S, Paek N C. 2012. STAY-GREEN and chlorophyll catabolic enzymes interact at light-harvesting complex II for chlorophyll detoxification during leaf senescence in *Arabidopsis*. *Plant Cell*, **24**, 507–518.
Schenk N, Schelbert S, Kanwischer M, Goldschmidt E E, Dormann P, Hortensteiner S. 2007. The chlorophyllases AtCLH1 and AtCLH2 are not essential for senescence-related chlorophyll breakdown in *Arabidopsis thaliana*. *FEBS Letters*, **581**, 5517–5525.
Shemer T, Harpaz-Saad S, Belausov E, Lovat N, Krokhin O, Spicer V, Standing K G, Goldschmidt E E, Eyal Y. 2008. *Citrus* chlorophyllase dynamics at ethylene-induced fruit color-break: A study of chlorophyllase expression, posttranslational processing kinetics, and in situ intracellular localization. *Plant Physiology*, **148**, 108–118.
Stincone A, Prigione A, Cramer T, Wamelink M M C, Campbell K, Cheung E, Olin-Sandoval V, Gruning N M, Kruger A, Alam M T, Keller M A, Breitenbach M, Brindle K M, Rabinowitz J D, Ralser M. 2015. The return of metabolism: Biochemistry and physiology of the pentose phosphate pathway. *Biological Reviews*, **90**, 927–963.
Tian Y Y, Wang H Y, Sun P, Fan Y G, Qiao M M, Zhang L X, Zhang Z Q. 2019. Response of leaf color and the expression of photoreceptor genes of *Camellia sinensis* cv. Huangjinya to different light quality conditions. *Scientia Horticulturae*, **251**, 225–232.
Tsuchiya T, Ohta H, Okawa K, Iwamatsu A, Shimada H, Masuda T, Takamiya K. 1999. Cloning of chlorophyllase, the key enzyme in chlorophyll degradation: Finding of a lipase motif and the induction by methyl jasmonate. *Proceedings of the National Academy of Sciences of the United States of America*, **96**, 15362–15367.
Wang F, Chen Y Z, Wang X P, You Z M, Chen C S. 2016. Leaf functional and photosynthetic characteristics in different leaves positions of tea plant. *Journal of Tea Science*, **36**, 77–84.
Wang K R, Du Y Y, Shao S H, Lin C, Ye Q, Lu J L, Lliang Y R. 2010. Development of specific RAPD markers for identifying albino tea cultivars 'Qiannianxue'and 'Xiaoxueya'. *African Journal of Biotechnology*, **9**, 434–437.
Wang S B. 2011. Study on the regularity of chlorophyll content in 'Anji baicha'. *Zhejiang Agricultural Sciences*, **6**, 1269–1272. (in Chinese)
Wang Y J, Hu X, Jin G, Hou Z W, Ning J M, Zhang Z Z. 2019. Rapid prediction of chlorophylls and carotenoids content in tea leaves under different levels of nitrogen application based on hyperspectral imaging. *Journal of the Science of Food and Agriculture*, **99**, 1997–2004.
Wei K, Wang L Y, Zhou J, He W, Zeng J M, Jiang Y W, Cheng H. 2012. Comparison of catechins and purine alkaloids in albino and normal green tea cultivars (*Camellia sinensis* L.) by HPLC. *Food Chemistry*, **130**, 720–724.
Wu Q J, Chen Z D, Sun W J, Deng T T, Chen M J. 2016. *De novo* sequencing of the leaf transcriptome reveals complex light-responsive regulatory networks in *Camellia sinensis* cv. Baijiguan. *Frontiers in Plant Science*, **7**, 332.
Wu Z J, Liu K Y, Zhang X, Tang Q H, Zeng L. 2024. *CsNYC1a* mediates chlorophyll degradation and albino trait formation in the Arbor-Type tea plant *Camellia nanchuanica*. *Journal of Agricultural and Food Chemistry*, **72**, 14087–14098.
Xu X F, Zhu H Y, Ren Y F, Ye Z H, Cai H M, Wan X C, Peng C Y. 2021. Efficient isolation and purification of tissue-specific protoplasts from tea plants (*Camellia sinensis* (L.) O. Kuntze). *Plant Methods*, **17**, 84.
Zhang C Y, Liu H R, Wang J Y, Li Y Y, Liu D D, Ye Y Y, Huang R, Li S J, Chen L, Chen J D, Yao M Z, Ma C L. 2024. A key mutation in magnesium chelatase I subunit leads to a chlorophyll-deficient mutant of tea (*Camellia sinensis*). *Journal of Experimental Botany*, **75**, 935–946.
Zhang C Y, Wang M H, Gao X Z, Zhou F, Shen C W, Liu Z H. 2020. Multi-omics research in albino tea plants: Past, present, and future. *Scientia Horticulturae*, **261**, 108943.
Zheng C H, Xu Z H, Wang Y Z, Zhang M M, Du K J, Li X J, Liu C P. 2023. Four *Ailanthus altissima* (Mill) swings varieties: Pigment compostion and distribution of leaves at different positions. *Chinese Agricultural Science Bulletin*, **32**, 56–65. (in Chinese)